*Applied Ocean Research* **14** (1992) 241–257

# Nonlinear oscillations, bifurcations and chaos in a multi-point mooring system with a geometric nonlinearity

**Oded Gottlieb* & Solomon C.S. Yim**

*Ocean Engineering Program, Oregon State University, Corvallis, Oregon 97331, USA*

(Received 9 December 1991; accepted 8 March 1992)

A taut multi-point mooring system with a large geometric nonlinearity under wave and current excitation is examined in this paper. The system is found to exhibit local instability and global bifurcations leading to complex nonlinear and chaotic responses. A semi-analytic method based on stability analyses of approximate solutions to the exact nonlinear system is shown to be an efficient predictor of bifurcations and chaos. Thus the method may supplant or significantly reduce the effort of a numerical parametric analysis for the strongly nonlinear ocean system.

*Key words:* mooring systems, nonlinear, stability, bifurcation, chaos.

## 1 INTRODUCTION

Complex nonlinear and chaotic responses have been recently observed in various numerical and approximate semi-analytical models of compliant offshore structures and mooring systems.[1–10] These systems are characterized by a unique equilibrium position (or single well potential), a strong nonlinearity described by a monotone increasing mooring restoring force, and by a fluid–structure interaction exciting force which couples the velocities of the structure with those of the field. System stability is governed by complex near resonant phenomena and sensitivity to initial conditions. Numerical investigations of systems which exhibit similar nonlinear properties have revealed complex behavior including coexisting periodic (harmonic, subharmonic and superharmonic) and aperiodic (quasiperiodic, chaotic) solutions defined by different initial conditions. A fundamental example of such systems is the symmetric and biased hardening Duffing equation.[11–13]

While weakly nonlinear systems have been studied extensively from both classical[14] and modern[15] approaches, complex single well potential systems with a strong nonlinearity are limited in their scope of analysis as they belong to a class of degenerate bifurcation problems. Two possible classical analytical methods of treating strong nonlinearities, where small perturbation solutions break down, are modified multiple scales[16] and the method of harmonic balance.[17] Both methods, applied to the hardening type Duffing equation, show good agreement with numerical solutions but are sensitive to order of approximation for a symmetric elastic configuration without a linear static term.[18,19] Stability analysis of system behaviour results in a local bifurcation map defining the regions of existence of the various nonlinear phenomena in parameter space. This analysis consists of perturbing an approximate solution and analyzing the resulting variational equation numerically by Floquet analysis[14] or by analytically evaluating the equivalent Hill's variational equation.[20] Stability analysis by both methods has been successfully employed on both hardening and softening Duffing equations.[17,21,22] Qualitative stability analysis can also be performed on autonomous systems in which the excitation is not time dependent.[14] This consists of finding all of the system's fixed points (or equilibrium solutions) and investigating their local stability by perturbation. This technique is employed in the analysis of quasi-statically formulated systems or as an alternative approach to analysis of time-averaged amplitude equations obtained by quantitative analysis.[15]

Ocean mooring systems include single and multi-point

*Present address: Parsons Lab, Building 48–213, MIT, Cambridge, MA 02139, USA.

Applied Ocean Research 0141-1187/92/$05.00

configurations.[23] Single-point moorings are characterized by curvature, material and hydrodynamic load nonlinearities[24] whereas multi-point systems or spread mooring systems incorporate an additional geometric nonlinearity associated with mooring line angles. The hydrodynamic excitation includes coupled nonlinear fluid–structure interaction drag and inertial components and requires separate treatment for small versus large bodies.[25] Small bodies (with respect to the flow wavelength) do not alter the incident flow, whereas large bodies change the characteristics of the flow field in the vicinity of the body and require knowledge of the scattered and radiated potentials in addition to the incident wave potential.[26] Consequently, the exciting forces on small bodies (e.g. semi-submersibles, articulated towers) can be directly incorporated into the system model via a semi-empirical relative motion Morison equation,[27] whereas large bodies (e.g. ships, floating production systems) require solution of the complete fluid–body boundary value problem or by formulation of approximate quasi-static maneuvering equations.[28,29] The quasi-static large body formulation can include additional constant descriptions of wind, current, second order (slow) wave drift forces[30] and memory effects.[28] A nonsteady gusting wind and first order (fast) random waves have also been added to the quasi-static models.[31] In a recent paper, Bernitsas and Chung[8] present a review of the approaches developed for single- and multi-point systems in the past four decades. The nonlinear elastic force of single cable line has been formulated by various methods. Examples are quasi-static formulation of semi-empirical relations for elastic rope,[32] catenary equations for chain,[24] and finite elements for steel cable.[33] An alternative is to incorporate a measured restoring force or its approximation. Examples of approximations by elementary functions are a piece-wise linear formulation,[34] an exponential function description[4] and a truncated power series described by a quartic polynomial.[35] Another single-point configuration, modeling coupled tanker-mooring tower motion, consists of a bi-linear formulation[2] and a least squares approximation of the restoring force resulting in a biased Duffing equation.[9] The geometric nonlinearity of multi-point systems has been exactly incorporated in two-point[8] and four-point systems[7] and by various approximations which are based on measured data.[4]

Numerical time domain simulation has been the primary tool for solution of both large[36] and small body configurations.[6] The harmonic balance method complemented by local stability analysis were applied to a single degree of freedom, geometrically nonlinear four-point mooring system[7] and to single-point systems modeled by quartic[35] and cubic polynomials.[9] Local autonomous system stability analysis was performed on quasi-static, three degree of freedom, large body models of single-[3,5] and two-point[8] mooring systems. Addition of nonsteady first and second order wave excitation,[31] was performed by numerical simulation of the time-dependent system for a given input parameter set. Local stability analysis was performed on the reduced time-averaged components of the wave excitation.[37] Another example of local stability analysis is the ship roll model. The roll restoring moment described by a quintic polynomial approximation was analyzed by multiple scales[38,39] and by an equivalent harmonic balance method.[40] Local stability analysis of steady state solutions by Floquet analysis revealed complex nonlinear and chaotic phenomena. However, the roll oscillator fundamentally differs from the mooring system as it is physically characterized by a double well potential (or a saddle connection). The description of the roll oscillator as a weakly nonlinear softening Duffing equation with additional weak nonlinear damping enables application of geometric methods[15] to obtain global stability results.[41] A detailed analysis[42] also portrays a capsize mechanism (escape from the well) not possible in the mooring problem.

Existing mooring systems analysis is portrayed by both complex numerical models incorporating both structural and hydrodynamic excitation or by idealized numerical or semi-analytical models where the nonlinearities are approximated and are in part described by their linearized or quasi-static representation. Due to their complexity, identification and control of system instabilities are not always attainable in the former models and require extensive parametric analysis, whereas the latter models are limited by their restrictive assumptions and do not always reveal true system behavior. Comparison of the complex phenomena obtained by the qualitative global analysis of the quasi-static analysis of single-[3,5] versus two-point moorings analysis[8] reveals the existence of similar singularities and bifurcations but detailed bifurcation analysis will be required to isolate and identify the various mechanisms governing system stability. Jiang, in a recent analysis of a single-point mooring system[10] found self-sustained oscillations which become chaotic when the system was subjected to an additional bias or periodic waves. Furthermore, evidence of strong subharmonic response and a period multiplying route to chaotic motion appears in numerical models of both large and small body ocean mooring models that are subjected to combined steady and fast motions.[6,10] These nonlinear solutions exist in a relatively narrow parameter space but their magnitude is greater than that of the coexisting harmonic response. As noted above, the multi-point mooring systems exhibit a variety of both structural and hydrodynamical nonlinearities. Consequently, in order to determine mechanisms governing system instabilities and sensitivity to initial conditions, a comprehensive understanding of system behaviour is needed. Examples of two fundamental topics for investigation are: (i) the influence of individual nonlinearities and the mechan-

isms governing system instabilities and sensitivity to initial condition, (ii) the relationship between constant and time-dependent excitation as depicted in the numerical[6] and perturbed quasi-static models incorporating constant/slowly varying and fast motions.[10,37] In order to address these questions the following system was chosen for analysis.

This paper describes the analysis of a floating structure connected to a symmetric multi-point mooring assembly. The system is forced by periodic waves in a steady current. In order to isolate the effect of geometric nonlinearity, linearized drag is employed and stiffness of a taut continuous form is assumed. Consequently, the validity of the model, which describes a strongly nonlinear mooring system constructed from linear spring elements, is restricted to small amplitude (linear) waves and higher order effects are assumed weak and incorporated into the co-linear current. In past analyses of ocean systems, nonlinearities including the restoring force were usually approximated by elementary functions such as polynomial or exponential functions. Results of analyses of these approximate systems could be misleading due to insufficient accuracy in the approximation and the strong sensitivity of the original systems. In this study, the exact analytical form of the nonlinear restoring is retained instead of employing approximating elementary functions. In order to quantitatively resolve system response under nonsteady conditions, a small body is chosen, thus eliminating the need to obtain a fundamental numerical solution. Global analysis by a Liapunov function approach results in a bounded solution set for small excitation. Although this result insures the existence of an attractor, it does not address coexistence or sensitivity to initial conditions which are pursued by local stability and global bifurcation analysis. Due to the complexity of the algebraic nonlinearity in the restoring force, the method of harmonic balance is utilized to obtain an approximate solution. Stability analysis of the variational equation proves the existence of multiple periodic solutions. Local stability analysis leads to global period doubling bifurcations and the onset of chaos. These analytical predictions are confirmed by numerical solutions of the exact system. Numerical simulations also show an underlying structure of multiple coexisting attractors, including saddle-node bifurcations (ultraharmonic resonances) and chaotic jumps (explosions) brought on by an abrupt loss of stability of a ultra-subharmonic solution.

## 2 SYSTEM MODEL

The multi-point mooring system considered (Fig. 1) is formulated as a single degree of freedom (surge), hydrodynamically damped and excited nonlinear oscillator. The equation of motion is derived based on equilibrium of geometric restoring forces and small body motion under wave and current excitation.[25]

$$m\ddot{X} + c\dot{X} + R(X) = F(\ddot{X}, \dot{X}, t) \tag{1a}$$

where

$$R(X) = k[X + b\,\mathrm{sgn}\,(X)] \times \left\{1 - \sqrt{\frac{d^2 + b^2}{d^2 + [X + b\,\mathrm{sgn}\,(X)]^2}}\right\} \tag{1b}$$

$$F(\ddot{X}, \dot{X}, t) = \lambda(u - \dot{X})|u - \dot{X}| + \mu(\dot{u} - \ddot{X}) + \rho\forall\dot{u} \tag{1c}$$

and

$m, c, k$ = system mass, structural damping and stiffness ($k = 2EA/\sqrt{(d^2 + b^2)}$, EA elastic cable force)

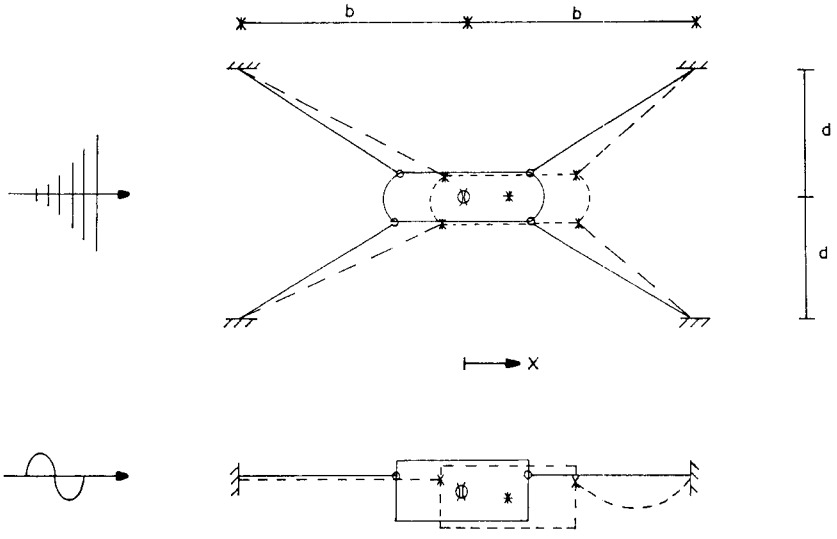


**Fig. 1.** Multi-point mooring assembly.

$\lambda, \mu$ = hydrodynamic viscous drag and added mass ($\lambda = 0{\cdot}5\rho S C_d$, $\mu = \rho \forall C_a$, $\rho$ water mass density)

$S, \forall$ = system projected drag area and displaced volume

$C_d, C_a$ = drag and inertia coefficients

$u(t)$ = time-dependent function of current and wave velocity: $u = u_0 + u_1 \sin(\omega t)$; $u_1 = u_1(a, \omega)$, where $u_0$ is the current magnitude and $a, \omega$ are the wave amplitude and frequency, respectively.

Note that $(\dot{})$ is the differentiation with respect to time and sgn $(X)$ denotes the sign of $X$.

A symmetric multi-point mooring system, based on taut linear elastic cables with zero tension when the system is unforced, yields an antisymmetric restoring force (Fig. 2(a)). Although the cables have linear elastic properties, the restoring force (stiffness) $R(x)$ may contain strong geometric nonlinearity depending on mooring angles. The stiffness nonlinearity can vary from a strongly nonlinear two-point system ($b = 0$) to an almost linear four point system ($b \gg d$).

The excitation force is based on small body theory with frequency-independent coefficients which assumes that the presence of the structure does not affect the wave field, hence waves propagating past the structure remain unmodified. This approach can be justified for slender body motion in the vertical plane (surge, heave, pitch) where the wavelength is large compared to the beam.[26] The hydrodynamic drag and inertia forces are based on superposition of wave and current velocities. The current is assumed to be steady, in line with the waves, and has a constant profile in the vertical direction.

A quadratic drag force is assumed to account for viscous effects on the body when the wave height is large compared to the beam of the structure. In order to isolate the influence of the geometric nonlinearity on the system, equivalent linearization of the quadratic drag force was performed.[43] The equivalent drag force coefficient was obtained by equating the average power of the linearized ($\lambda_{lin}$) and the quadratic ($\lambda$) drag force over one wave cycle [$\lambda_{lin} = \lambda_{lin}(\lambda; u_0, u_1) : \lambda_{lin}(u_0 = 0) = 8\lambda/3\pi$].

Thus, for bodies with limited interaction with the sea surface, the added mass and viscous damping coefficients are assumed to be independent of the excitation frequency.

Rearranging and normalizing ($x = X/d$) the equation of motion (eqn (1)) yields the following first order autonomous system:

$$\dot{x} = y \qquad \dot{y} = F(\theta; f_0, f_1, \omega, \phi) - R(x; \alpha, \beta) - \delta y$$
$$\dot{\theta} = \omega \tag{2a}$$

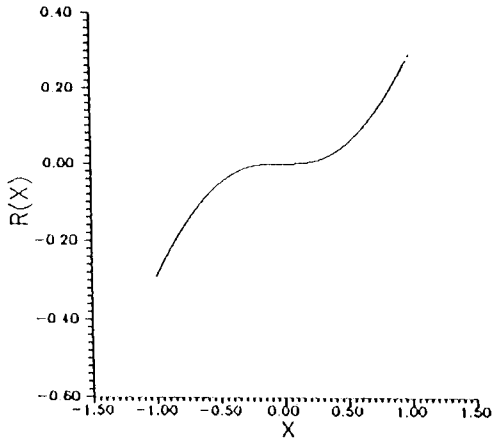


(a)

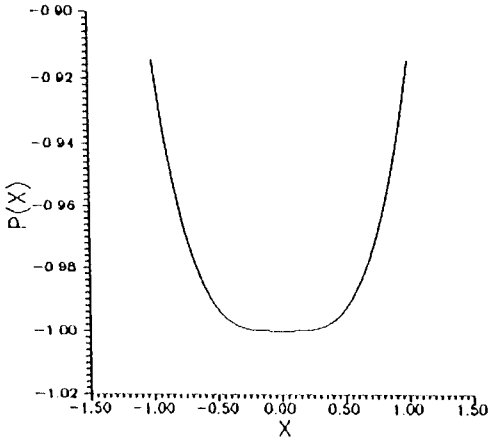


(b)

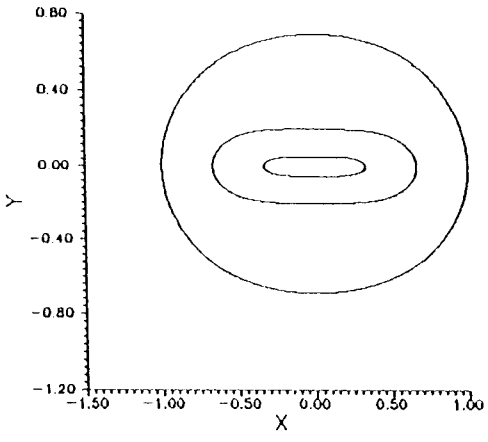


(c)

**Fig. 2.** Hamiltonian system: (a) restoring force, (b) potential, (c) phase plane.

where

$$\theta(t) = \omega t + \phi$$

$$R(x) = \alpha[x + \beta \operatorname{sgn}(x)] \times \left\{ \frac{1}{\sqrt{1+\beta^2}} - \frac{1}{\sqrt{1 + [x + \beta \operatorname{sgn}(x)]^2}} \right\} \quad (2b)$$

$$F(\theta) = f_0 - f_1 \sin(\theta) \quad (2c)$$

and

$$\alpha = \frac{k}{m+\mu}, \qquad \beta = \frac{b}{d}, \qquad \delta = \frac{c + \lambda_{\text{lin}}}{m+\mu}$$

$$f_0 = \frac{\lambda_1 u_0}{m+\mu}$$

$$f_1 = \frac{\rho \nabla u_1}{m+\mu} \sqrt{\omega^2 (1 + C_a)^2 \frac{1}{4} C_{dl}^2 \left(\frac{\nabla}{S}\right)^2}$$

$$\varphi = \arctan\left[2\omega \frac{(1 + C_a)}{C_{dl}} \frac{\nabla}{S}\right]$$

where $C_{dl}$ = linearized drag coefficient.

## 3 GLOBAL ATTRACTION

The system (eqn (2)) does not have any fixed points in three-dimensional space $(x, y, \theta)$ because $d\theta/dt = \omega$ in (eqn (2a)). However, a unique equilibrium position $[(x, y)_e = (0, 0)]$ in two-dimensional space $(x, y)$ can be determined via the associated integrable Hamiltonian system which yields a phase diagram of stable centers (Fig. 2(c)).

$$y = \sqrt{2[P(x_0) - P(x)]} \quad (3a)$$

where $P(x) = \int R(x)dx$ is the potential energy of the system (Fig. (2(b))

$$P(x) = \alpha \left\{ \frac{[x + \beta \operatorname{sgn}(x)]^2 - \beta^2}{2\sqrt{1+\beta^2}} - \sqrt{1 + [x + \beta \operatorname{sgn}(x)]^2} \right\} \quad (3b)$$

and $P(x_0)$ is a function of initial conditions calculable from the invariant Hamiltonian energy $H(x, y)$:

$$H(x, y) = \tfrac{1}{2} y^2 + P(x; \alpha, \beta) \quad (3c)$$

Local stability analysis[14] of the unforced system $(f_0, f_1 = 0)$ yields a unique asymptotically stable sink at the origin. This analysis consists of calculating the eigenvalues describing a nontrivial solution of the linearized system near the origin which results in a structurally stable sink.

$$e_{1,2} = \tfrac{1}{2} \left\{ -\delta \pm \sqrt{\delta^2 - 4\alpha\beta^2 (1+\beta^2)^{-3/2}} \right\}$$

Excitation of the system by current alone $(f_0 \neq 0, f_1 = 0)$ creates a bias or a shift in the location of the stable attractor $((x, y)_e = (c, 0)$ where $R(c) = f_0/\alpha)$ of the response. However, with the addition of harmonic wave excitation the hyperbolic fixed point (sink) becomes a hyperbolic closed orbit (limit cycle). Although the limit cycle loses the circularity of the sink, it is anticipated by the invariant manifold theorem to retain its stable characteristics for small excitation.[15] In order to validate and quantify the qualitative results of local analysis, global stability of the system is performed by a Liapunov function approach.[44]

For the undamped (Hamiltonian) system, a weak Liapunov function $V(x, y)$ with $V(0, 0) = 0$ at $(x, y)_e = (0, 0)$, and $dV/dt \equiv 0$, can be found by adding a constant term $\sqrt{(1+\beta^2)}$ to the Hamiltonian energy (eqn (3c)). Thus the origin is neutrally stable.

Modification of $V(x, y)$ to account for damping, results in a strong Liapunov function.

$$V(x, y) = \tfrac{1}{2} y^2 + \alpha \left[ P(x) + \sqrt{1+\beta^2} \right] + \nu(x, y + \tfrac{1}{2}\delta x^2) \quad (4a)$$

and

$$\dot{V} = y\dot{y} + \alpha \left[ \frac{dP(x)}{dx} \dot{x} \right] + \nu(y\dot{x} + x\dot{y} + \delta x\dot{x})$$
$$= -\nu[\alpha x R(x)] - (\delta - \nu) y^2 \quad (4b)$$

Choosing $\nu$ (in eqn (4a, b)) sufficiently small $(0 < \nu < \delta)$ results in a globally stable unforced system where $V(x, y)$ is positive definite and $dV/dt \leq 0$.

The characteristics of the biased system with current alone remain unchanged. The biased system describes a quasi-statically formulated single degree of freedom mooring system. Consequently, this result implies the existence of an attractive set for multi-point mooring systems driven by steady excitation representative of superimposed constant forcing.

In order to confirm global stability of the harmonically excited system, differentiation of the Liapunov function is performed along solution curves of the forced system.[45]

$$\dot{V} = -\nu\alpha x R(x) - (\delta - \nu) y^2 + (f_0 - f_1 \sin\theta)(\nu x + y)$$
$$\leq -\nu\alpha x R(x) - (\delta - \nu) y^2 + |\nu f_0 x| + |f_0 y| + |\nu f_1 x| + |f_1 y| \quad (4c)$$

Thus, for small $f_0$ and $f_1$, and in the neighborhood of $(x, y) = (0, 0)$, solutions of the system remain bounded $(dV/dt \leq 0)$, and the limit cycles are globally stable for small excitation. Strong excitation and coexistence of solutions will be addressed by local stability analysis.

## 4 HARMONIC SOLUTION AND FREQUENCY RESPONSE

Investigation of system response under wave and current and under wave excitation alone is similar to analysis of a system with unsymmetric and symmetric elastic functions, respectively. In both cases the T periodic solution can be approximated by a finite Fourier series expansion of the following form:

$$x_0(t) \simeq \sum_k A_k \cos\left[k(\omega t + \Phi)\right] \tag{5a}$$

where

$$x_0(t) \neq -x_0\left(t + \frac{T}{2}\right);$$
$$k = 0, 1, 2, \ldots, K(\text{unsymmetric})$$
$$x_0(t) = -x_0\left(t + \frac{T}{2}\right);$$
$$k = 1, 3, 5, \ldots, K(\text{symmetric}) \tag{5b}$$

and $K$ is the desired order of approximation.

The unsymmetric solution includes both even and odd harmonics whereas the symmetric solution consists of only odd harmonics. Note that although the system response is associated with the excitation characteristics of system (i.e. wave excitation with or without current), the two types of excitation can have both symmetric and unsymmetric solution forms.

Due to the complex strong nonlinearity of the restoring force (eqn (2b)), the harmonic balance method is employed. The approximate solution (eqn (5)) is substituted into the system (eqn (2)). After rearranging and squaring, the harmonic and constant coefficients are equated separately to zero. The original system of nonlinear differential equations is replaced by a set of nonlinear algebraic equations:

$$G_i(A_k, \Phi) = 0 \tag{6a}$$

where

$$i = 1, 2, \ldots, N$$
$$\begin{cases} N = k + 2; & k = 0, 1, \ldots, K(x(t) - \text{unsymmetric}) \\ N = \dfrac{k+3}{2}; & k = 1, 3, \ldots, K(x(t) - \text{symmetric}) \end{cases} \tag{6b}$$

(see Appendix for details).

Solutions of this set (eqn (6)) are obtained using an iterative Newton-Raphson procedure. Frequency response curves (Fig. 3) are generated numerically by solving a set of nonlinear algebraic equations for the unknown amplitudes ($A_k$) and phase ($\Phi$).

The response frequency of the Hamiltonian system $\omega_n = 2\pi/T$, is directly computed by integrating the Hamiltonian phase plain to obtain the response period $T = 4\int y^{-1}\mathrm{d}x$ where $y$ is given by eqn (3a). The

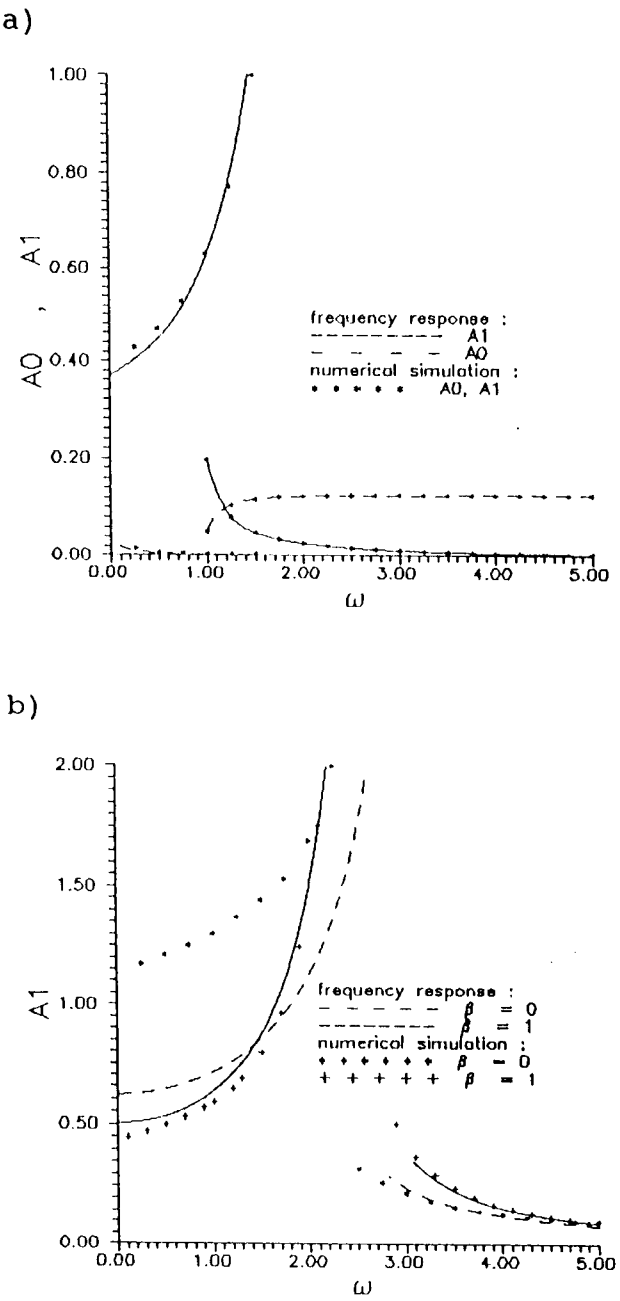


**Fig. 3.** Frequency response: (a) wave and current ($\alpha = 10$, $\delta = 0{\cdot}5$, $f_0 = 0{\cdot}01$, $f_1 = 0{\cdot}1$); (b) wave ($\alpha = 10$, $\delta = 0{\cdot}01$, $f_0 = 0, f_1 = 2$).

integral solution serves as an initial measure of accuracy for determining the resolution of the approximate solution from which the required order of approximation ($K$) is determined. The integral form of the frequency response of the Hamiltonian system ('backS > 'backbone' curve) can be used to characterize the degree of nonlinearity (Fig. 4). As noted previously, the nonlinearity is strong for large mooring angles ($\beta < 1$) and small displacements. It also serves as a measure of the accuracy of the approximate stability curves describing the primary resonance jump phenomenon or cyclic fold bifurcation.[46]

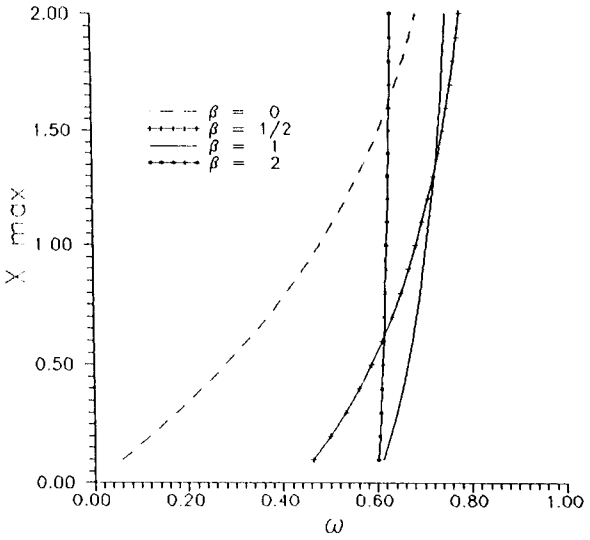


**Fig. 4.** Degree of geometric nonlinearity ($\alpha = 1$, $\delta = 0$, $f_0 = 0$, $f_1 = 0$).

Numerical simulations of the system were performed using a Runge-Kutta integration scheme where error control was achieved via the passage of the response through the exact fixed equilibrium point. The results show good agreement with low order approximations under wave and current excitation $[(i,k) = (3,1)]$ (Fig. 3(a)) and under wave excitation along $[(i,k) = (2,1)]$ (Fig. 3(b)). The low order (one term) approximation of a four-point system under wave excitation is sufficient for a large range of parameter conditions particularly for $\beta \approx 1$, but more terms are needed to correctly model the response of a two-point system ($\beta = 0$), near the primary resonance and in the low frequency secondary resonance range (Fig. 3(b)). It should be noted that the application of harmonic balance to a strong nonlinear systems requires the calculation of an error term (e.g. ratio of amplitude norm of two consecutive approximations: $\Sigma A_k^2/\Sigma A_{K+1}^2$) in order to determine solution convergence.

The expansion of the given restoring force (eqn (2b)) in a least squares sense yields a polynomial with odd components which is without a linear term for $\beta = 0$. The sensitivity of the approximate solution to the order of the approximation is similar to that of the Duffing equation without a linear term.[18]

## 5 STABILITY ANALYSIS AND EXISTENCE OF PERIOD DOUBLING

Local stability of the approximate solution was determined by considering a perturbed solution $x(t) = x_0(t) + \epsilon(t)$, where $x_0(t)$ is an approximate solution given by (eqn (5)) and $\epsilon(t)$ is a small perturbation. Substituting $x(t)$ in (eqn (2)) and simplifying the resulting equation leads to a nonlinear variational equation.

$$\ddot{\epsilon} + \delta\dot{\epsilon} + \alpha G[\epsilon; x_0(t)] = 0 \tag{7a}$$

where

$$G(\epsilon) = \frac{\epsilon}{\sqrt{1+\beta^2}} - \left\{ \frac{x_0 + \epsilon + \beta\,\mathrm{sgn}\,(x_0)}{\sqrt{1 + [x_0 + \epsilon + \beta\,\mathrm{sgn}\,(x_0)]^2}} - \frac{x_0\beta\,\mathrm{sgn}\,(x_0)}{\sqrt{1 + [x_0 + \beta\,\mathrm{sgn}\,(x_0)]^2}} \right\} \tag{7b}$$

Linearizing the variational (eqn (7b)) yields a linear ordinary differential equation with a periodic coefficient function $H[x_0(t)] = H[x_0(t+T)]$.

$$\ddot{\epsilon} + \delta\dot{\epsilon} + \alpha H[x_0(t)]\epsilon = 0 \tag{8a}$$

where

$$H(x_0) = (1+\beta^2)^{-1/2} - \{1 + [x_0 + \beta\,\mathrm{sgn}\,(x_0)]^2\}^{-3/2} \tag{8b}$$

Expanding $H(x_0)$ in a Fourier series $H(\Theta)$, leads to a general Hill's variational equation, which after substituting the solution (eqn (5)) into eqn (8) yields:

$$\ddot{\epsilon} + \delta\dot{\epsilon} + \alpha H[\Theta(t)]\epsilon = 0 \tag{9a}$$

where

$$H(\Theta) = \frac{a_0}{2} + \sum_n a_n \cos n\Theta \tag{9b}$$

and

$$\Theta(t) = \omega t + \phi + \Phi$$

$$a_n = \frac{2}{\pi}\int_0^{\pi} H(\Theta)\cos(n\Theta)\,\mathrm{d}\Theta$$

$$n = \begin{cases} 1,2,3,\ldots,K & [x(t) - \text{unsymmetric}] \\ 2,4,6,\ldots,K & [x(t) - \text{symmetric}] \end{cases}$$

Note that the approximation of the periodic coefficient in (eqn (8b)) by (eqn (9b)) is sensitivie to $\beta$. Both $H(x_0)$ and $H(\Theta)$ retain a singularity at $H(x_0 = 0) = \beta^2(1+\beta^2)^{(-3/2)}$ and for $x_0 > \pi$, $H(x_0)$ is asymptotic to $\sqrt{(1+\beta^2)}$ (Fig. 5).

The even and odd components in the Hill's equation are associated with the symmetric and unsymmetric solution forms and are related to the harmonic components of periods $T$ and $T/2$. The particular solution to the variational equation, $\epsilon = \exp(\dot{\zeta}t)Z(t)$, can be found by Floquet theory[47] with $Z(t) = Z(t+T)$ and $Z(t) = Z(t+T/2)$ for the symmetric solution form with only even components. The unsymmetric solution results in non-zero odd harmonic components with a period doubled solution form $Z(t) = Z(t+2T)$ in eqn (9b).

A low order two-term solution, $x_0(t) = A_0 + A_1\cos(\Theta)$ corresponding to response of wave

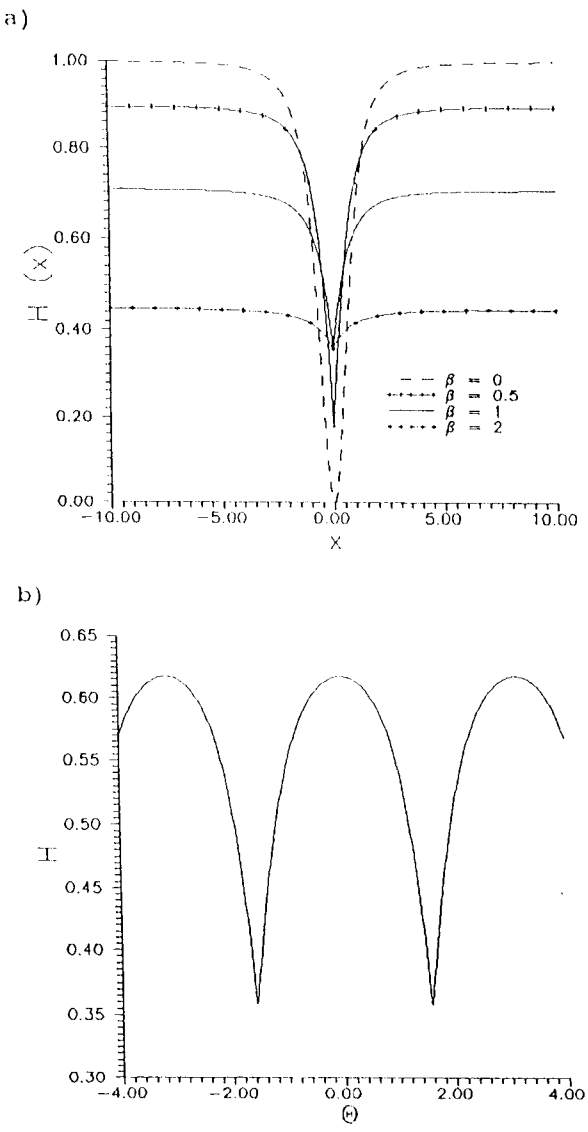


**Fig. 5.** Hill's variational function: (a) $H(x)$ (eqn (8b)); (b) $H(\Theta)$ (eqn (9b)).

and current excitation, results in an equivalent variation which defines the $Z(t) = Z(t+T)$ first order unstable region. As shown in Fig. 6(a) and (b), these regions coincide with vertical tangent points of the primary resonance on the frequency response curve. The boundaries of the unstable region are obtained by applying the harmonic balance method to the Hill's equation (eqn (9)) for $\epsilon(t)$ at the stability limit ($\dot{\zeta} = 0$).

$$\omega^2 = \frac{1}{2a_0}\left[\alpha(a_0^2 - a_1^2) - \delta^2 a_0 \pm \sqrt{\delta^4 a_0^2 + 2\alpha\delta^2(a_1^2 - a_0^2) + \alpha^2(a_1^2 - a_0 a_2)^2}\right] \tag{10a}$$

For the undamped system, $\delta = 0$, eqn (10a) simplifies to $\omega \approx \sqrt{(\alpha a_0/2)}$.

The lowest order instability of the solution form

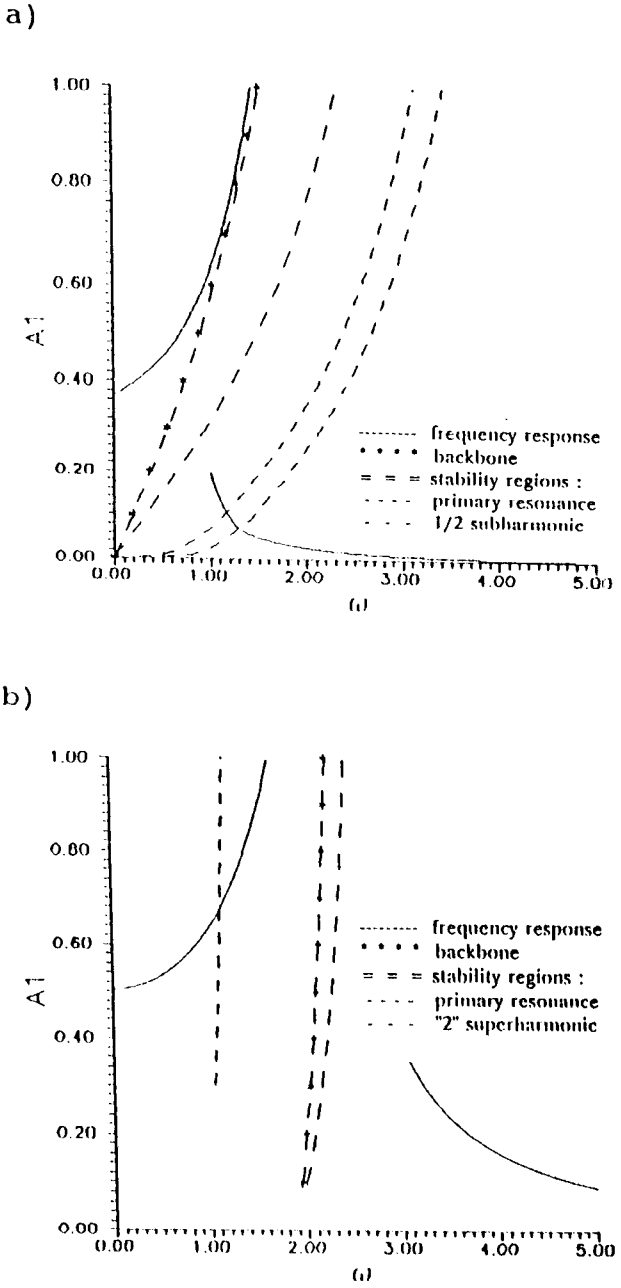


**Fig. 6.** Stability diagram: (a) wave and current ($\alpha = 10$, $\beta = 0$, $\delta = 0{\cdot}01$, $f_0 = 0{\cdot}01$, $f_1 = 0{\cdot}1$); (b) wave ($\alpha = 10$, $\beta = 1$, $\delta = 0{\cdot}01, f_0 = 0, f_1 = 2$).

$Z(t) = Z(t+2T)$ is obtained by inserting the period doubled $\epsilon(t) = b_{1/2}\cos(\Theta/2)$ into eqn (9) resulting in the boundaries of the first '1/2' subharmonic region (Fig. 6(a)).

$$\omega^2 = 2\left[\alpha a_0 - \delta^2 \pm \sqrt{\delta^4 - 2\alpha\delta^2 a_0 + \alpha^2 a_1^2}\right] \tag{10b}$$

For the undamped system, $\delta = 0$, eqn (10b) simplifies to $\omega \approx \sqrt{(2\alpha a_0)}$.

As noted previously, symmetric solutions such as $x_0(t) = A_1\cos\Theta$, corresponding to response of only wave excitation, do not exhibit a period doubling

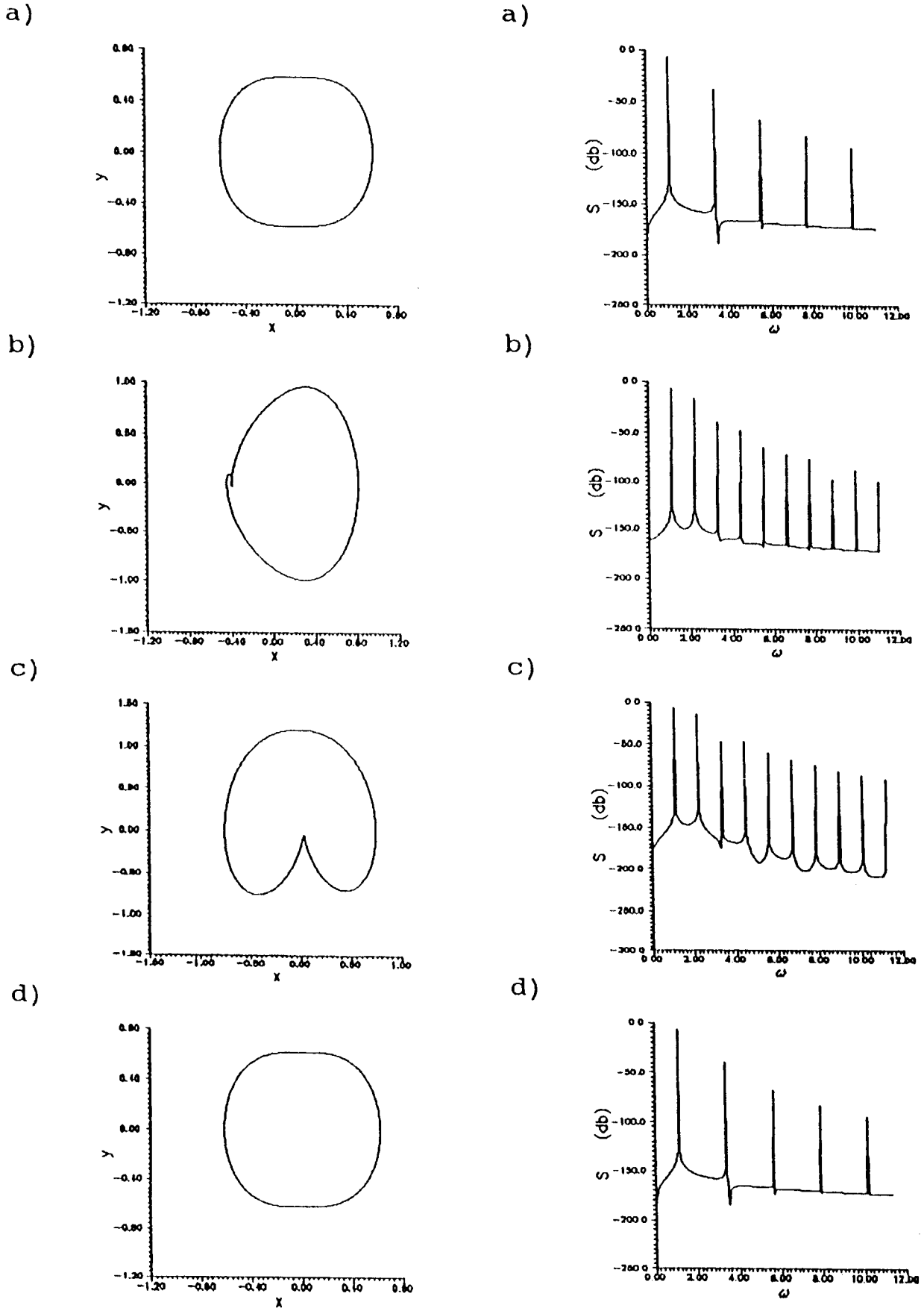


**Fig. 7.** Symmetry loss (phase space, power spectra) ($\alpha = 10, \beta = 1, \delta = 0{\cdot}01, f_0 = 0, f_1 = 2$; (a) $\omega = 1{\cdot}09$, (b) $\omega = 1{\cdot}10$, (c) $\omega = 1{\cdot}12$, (d) $\omega = 1{\cdot}13$).

phenomenon $Z(t) \neq Z(t+2T)$ but determine secondary resonances in which the $Z(t) = Z(t+T/2)$ solution loses stability. This instability is obtained by inserting the unsymmetric solution form $\epsilon(t) = b_0 + b_2 \cos(2\Theta)$ into eqn (9), yielding an approximate order 2 superharmonic region (Fig. 6(b)).

$$\omega^2 = \frac{1}{8a_0}\left[\alpha(a_0^2 - a_2^2) - \delta^2 a_0 \pm \sqrt{\delta^4 a_0^2 + 2\alpha\delta^2(a_2^2 - a_0^2) + \alpha^2(a_2^2 - 2a_0a_4)^2}\right] \tag{10c}$$

For the undamped system, $\delta = 0$, eqn (10c) simplifies to $\omega \approx \sqrt{(\alpha a_0/8)}$.

The stability loss of the symmetric solution is portrayed in the emergence of an unsymmetric solution $x_0(t) = A_0 + A_1 \cos(\Theta) + A_2 \cos(2\Theta)$, which when inserted in the variational equation, yields a period doubled solution $Z(t) = Z(t+2T)$ similar to the unsymmetric solution. This period doubling is associated with the appearance of subharmonics in the superharmonic domain (ultra-subharmonics).

Similar analysis of the 1/2 subharmonic[19] and the $k/2$ ($k$ odd) ultra-subharmonic resonance show the possible existence of a $4T$ periodic solution. Thus the general Hill's equation suggests the possible cascade of period doubling bifurcations.

## 6 BIFURCATIONS AND THE ONSET OF CHAOS

The approximate regions of bifurcation of the exact system can be determined by the intersections of the frequency response curve $[A_k = A_k(\omega)]$ and the stability regions of the approximate solution eqn (10), which are derived from the Hill's variational equation. As shown in Fig. 6(a), the stability region for the system under wave excitation with a weak current is that of period doubling of the unsymmetric solution. On the other hand, for the system under wave excitation alone, the stability boundary corresponds to loss of symmetry of the symmetric solution (Fig. 6(b)).

Loss of symmetry of the solution can be observed via the phase portraits $[y(x)]$ and power spectra $[S(\omega)]$ of the response. Since the exact system (eqn (2)) has solution forms $(x, y, \Theta)$ and $(-x, y, \Theta + \pi/\omega)$, therefore, if an orbit $[x(t), y(t)]$ exists it is either self similar $[x(t), y(t) = -x(t+\pi/\omega), -y(t+\pi/\omega)]$ or it has a coexisting orbit $[-x(t+\pi/\omega), -y(t+\pi/\omega)]$. The breaking of the symmetric solution in an unsymmetric solution occurs with variation of excitation frequency in the parameter space predicted by eqn (10c). The loss of symmetry, shown in Fig. 7(a) and (b), can be observed via the phase portrait and with the emergence of even harmonics in the power spectra of the non-symmetric solution. However, as the excitation frequency sweeps past the even harmonics disappear and the response again becomes symmetric (Fig. 7(d)).

As shown in Fig. 8, the symmetry bifurcation or dynamic symmetry breaking[13] consists of a transition from a self similar (symmetric) solution to two coexisting period $T$ partner orbits. Note that coexisting solutions are defined by different initial conditions in the same parameter space. Another consequence of symmetry[45] is that unsymmetric subharmonics of period $nT$ will always occur in multiples. This is portrayed with the phase plane and Poincaré map $[Y_p(X_p)]$ of a $5T$ ultra-subharmonic where unsymmetric subharmonics coexist (Fig. 9(a) and (b)) whereas a self-similar subharmonic will occur singly (Fig. 9(c)).

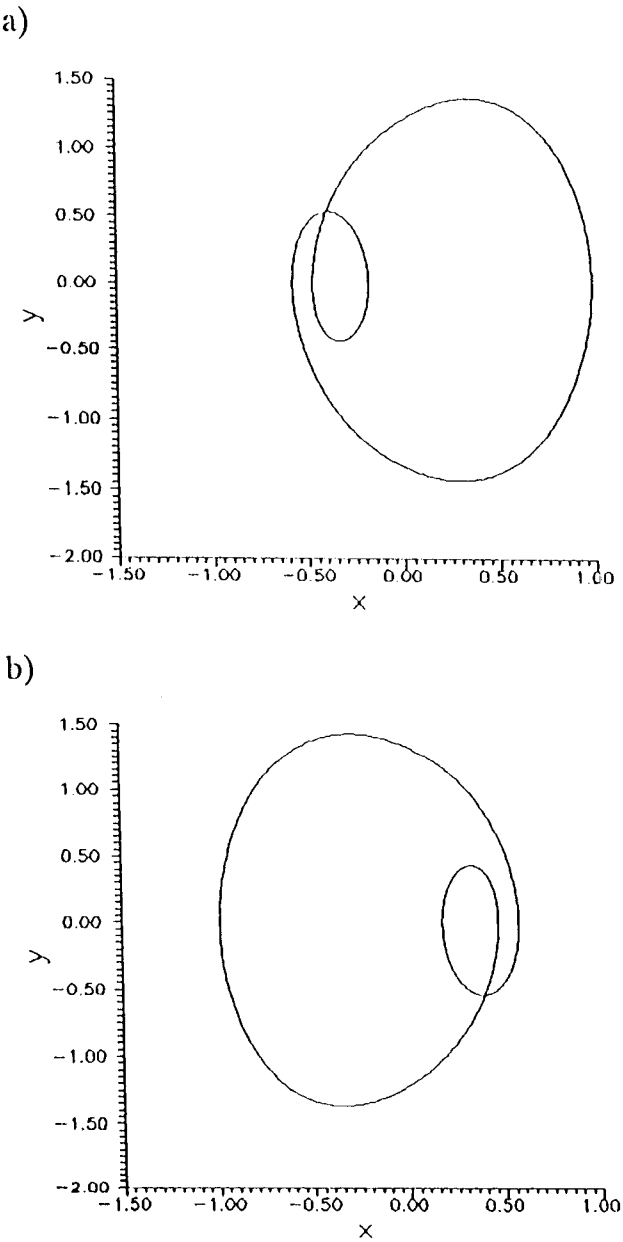


**Fig. 8.** Nonsymmetric period $T$ partner orbits (phase plane) ($\alpha = 10$, $\beta = 1$, $\delta = 0{\cdot}01$, $f_0 = 0$, $f_1 = 2$, $\omega = 1{\cdot}11$); initial conditions $[x(0), y(0)]$; (a) $[0, 0]$, (b) $[1, 1]$.

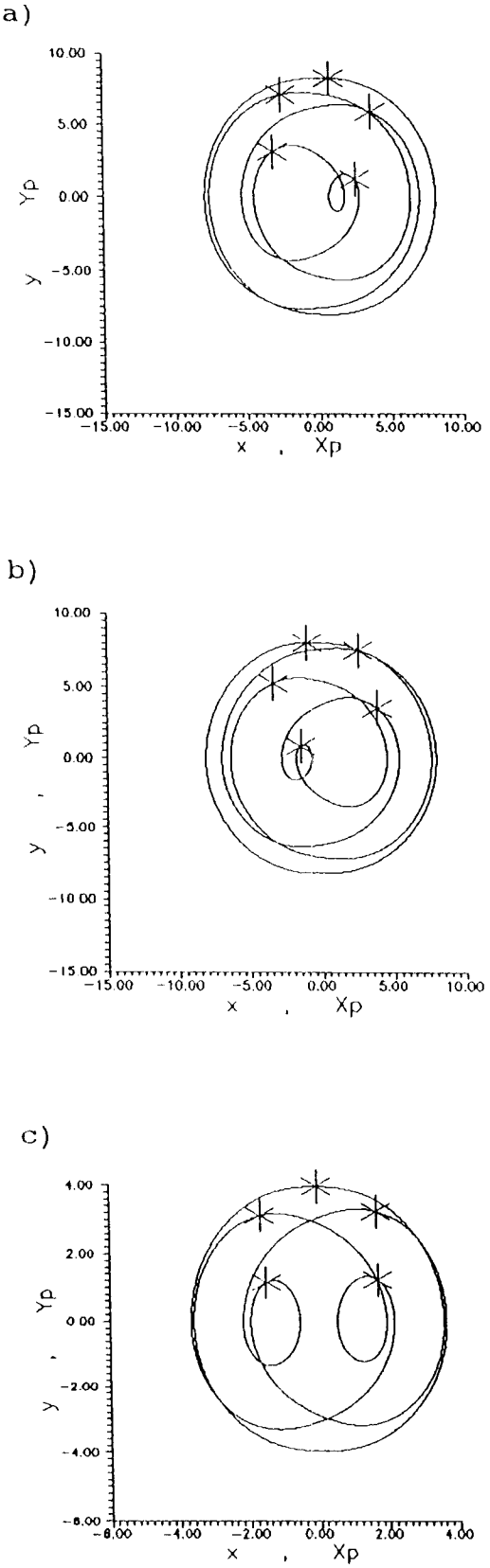


**Fig. 9.** Nonsymmetric partner orbits and self-similar 5T subharmonics (phase plane, Poincaré Map) ($\alpha = 1$, $\beta = 0$, $\delta = 0{\cdot}01$, $f_0 = 0$, $f_1 = 2$, $\omega = 1{\cdot}125$) initial conditions $[x(0)\ y(0)]$: (a) $[0,0]$, (b) $[-1,0]$ ($\alpha = 1$, $\beta = 1$, $\delta = 0{\cdot}01$, $f_0 = 0, f_1 = 2$, (c) $\omega = 1{\cdot}3$).

Application of stability analysis to the system can also reveal the type of local bifurcations causing loss of stability, i.e. saddle-node or pitchfork bifurcations.[15] This can be shown by calculation of the eigenvalues of the monodromy matrix associated with the fundamental solution of the linearized variational equation. The eigenvalues $E$ (or Floquet multipliers as $\xi(t + T/2) = E\xi(T)$) characterize the stability of the perturbed solution $|E| < 1$. Loss of stability can be obtained through $E = 1$ (saddle-node) or $E = -1$ (pitchfork). The eigenvalues are obtained by numerically integrating the variational equation (eqn (8)) over time (0 to $T/2$).[14]

Cascade of period doubling or the range of stability of the $2^nT$ limit cycle, can also be obtained by numerically integrating the linearized variation equation (eqn (8)) over time (0 to $2^nT$). Thus, the magnitude of the eigenvalues determines global period doubling [38,39] and verifies the validity of the stability regions previously determined directly (subharmonic) or through loss of symmetry of the response (ultra-subharmonic). The period doubling ($2T$) of the unsymmetric solution which further bifurcates into a $4T$ solution, occurs with an increase of excitation frequency in the parameter space predicted by eqn (10b,c) of the unsymmetric and symmetric configurations respectively. This behavior is shown in Fig. 10 for the case with wave and current excitation, and in Fig. 11 for wave excitation alone. If the period doubling sequence is infinite with a finite accumulation point, the resulting motion is chaotic. Thus, local stability analysis can identify regions of global bifurcation with universal characteristics.[48]

Using the semi-analytical procedure discussed above as a guide for numerical search in the parameter space, various types of responses of the exact system are identified. These responses consists of coexisting multiple periodic solutions, period doubling cascades and explosions leading to chaotic attractors. The explosion[12] (or crisis) is characterized by contraction of a period $3T$ limit cycle leading to an abrupt change to a chaotic attractor which becomes transient before settling to a regular solution.[49] Selected system responses are demonstrated here via their steady state phase portraits, Poincaré plots and power spectra. Figure 12 shows coexisting periodic solutions of symmetric $T$, 2 partner $2T$ and a self-similar $5T$ obtained for various initial conditions. Note that the magnitude of the subharmonic response is more than twice the size of the coexisting harmonic solution. A chaotic attractor corresponding to an infinite period doubling cascade is shown in Fig. 13 and a chaotic attractor corresponding to explosions is shown in Fig. 14.

## 7 CONCLUSIONS

Complex nonlinear and chaotic responses are predicted and found in a geometrically nonlinear taut multi-point

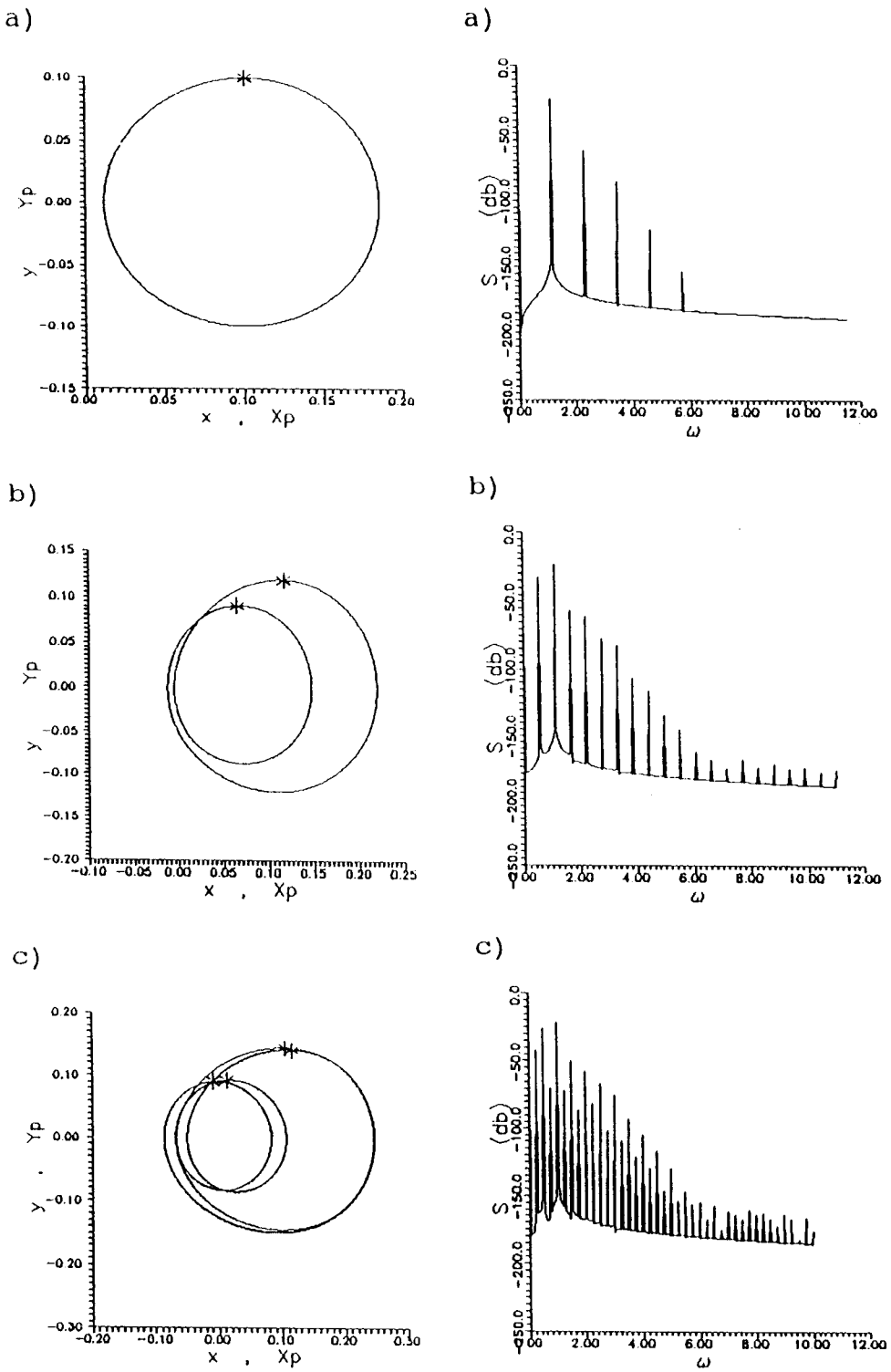


**Fig. 10.** Period doubling (phase plane, power spectra) ($\alpha = 10, \beta = 0, \delta = 0{\cdot}01, f_0 = 0.01, f_1 = 0{\cdot}1$; (a) $T$: $\omega = 1{\cdot}26$, (b) $2T$: $\omega = 1{\cdot}24$, (c) $4T$: $\omega = 1{\cdot}23$).

mooring system, which is globally stable under small wave and current excitations. Analysis of local bifurcations consisting of symmetry loss and period doubling, leads to global bifurcations and choas. Results show multiple coexisting solutions and existence of chaotic explosions which could not be predicted by equivalent linearization methods. They also indicate a possible underlying structure to the nonlinear phenomena where period doubling bifurcations and further explosions are found intersecting the superharmonic resonances of the ocean system.

A semi-analytic method describing local and global

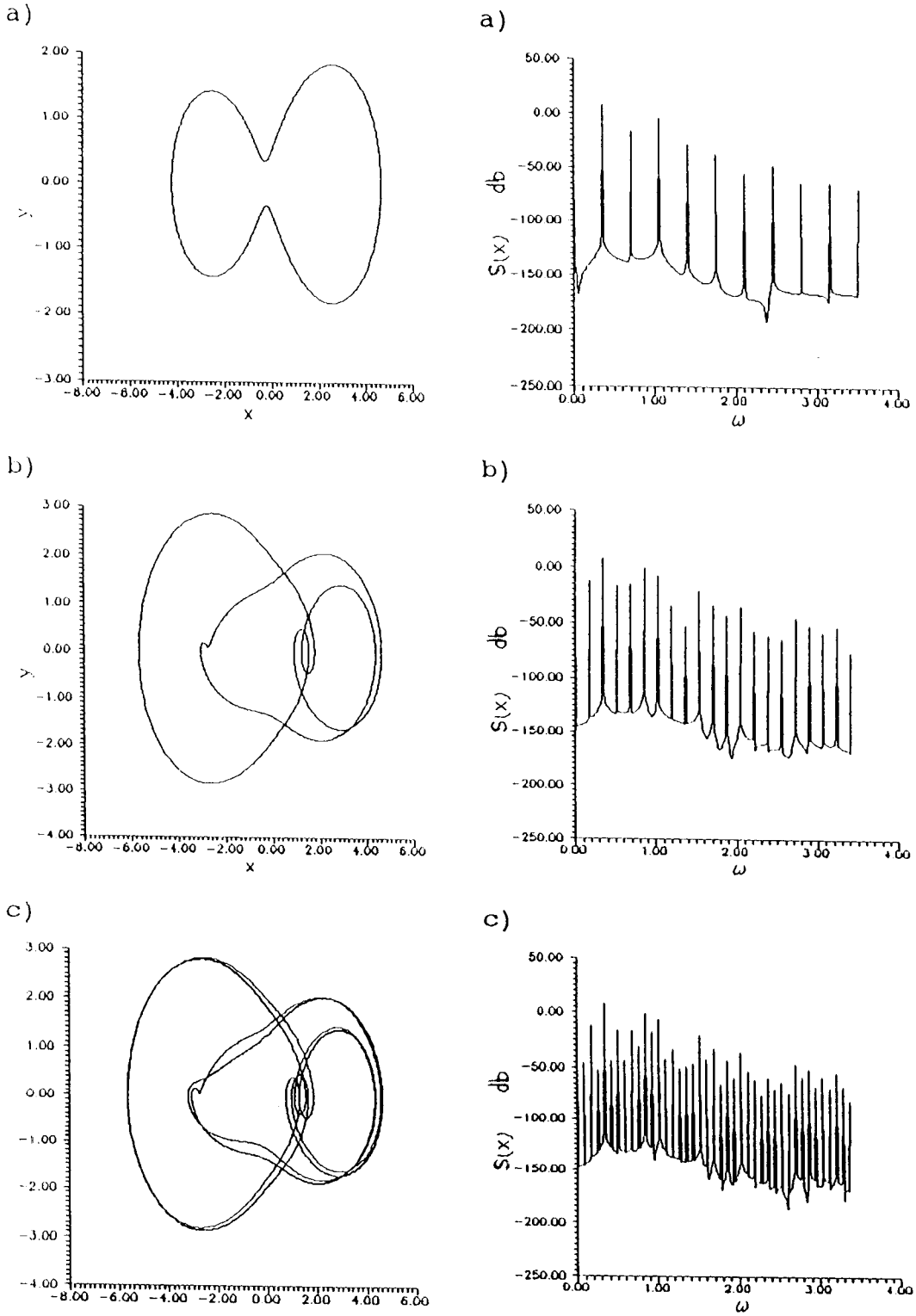


**Fig. 11.** Period doubling (phase plane, power spectra) ($\alpha = 10, \beta = 0, \delta = 0{\cdot}01, f_0 = 0, f_1 = 2$; (a) $T$: $\omega = 0{\cdot}35$, (b) $2T$: $\omega = 0{\cdot}34$, (c) $4T$: $\omega = 0{\cdot}337$).

bifurcations of the system characterized by an exact form of the geometric nonlinearity is derived and verified numerically. The method incorporates stability analysis of a low-order system response, approximated by the method of harmonic balance, leading to stability curves defining symmetry loss and period doubling in parameter space.

The characteristics of the external excitation determine the domain of existence for the nonlinear phenomena. A biased and harmonic excitation, generated by

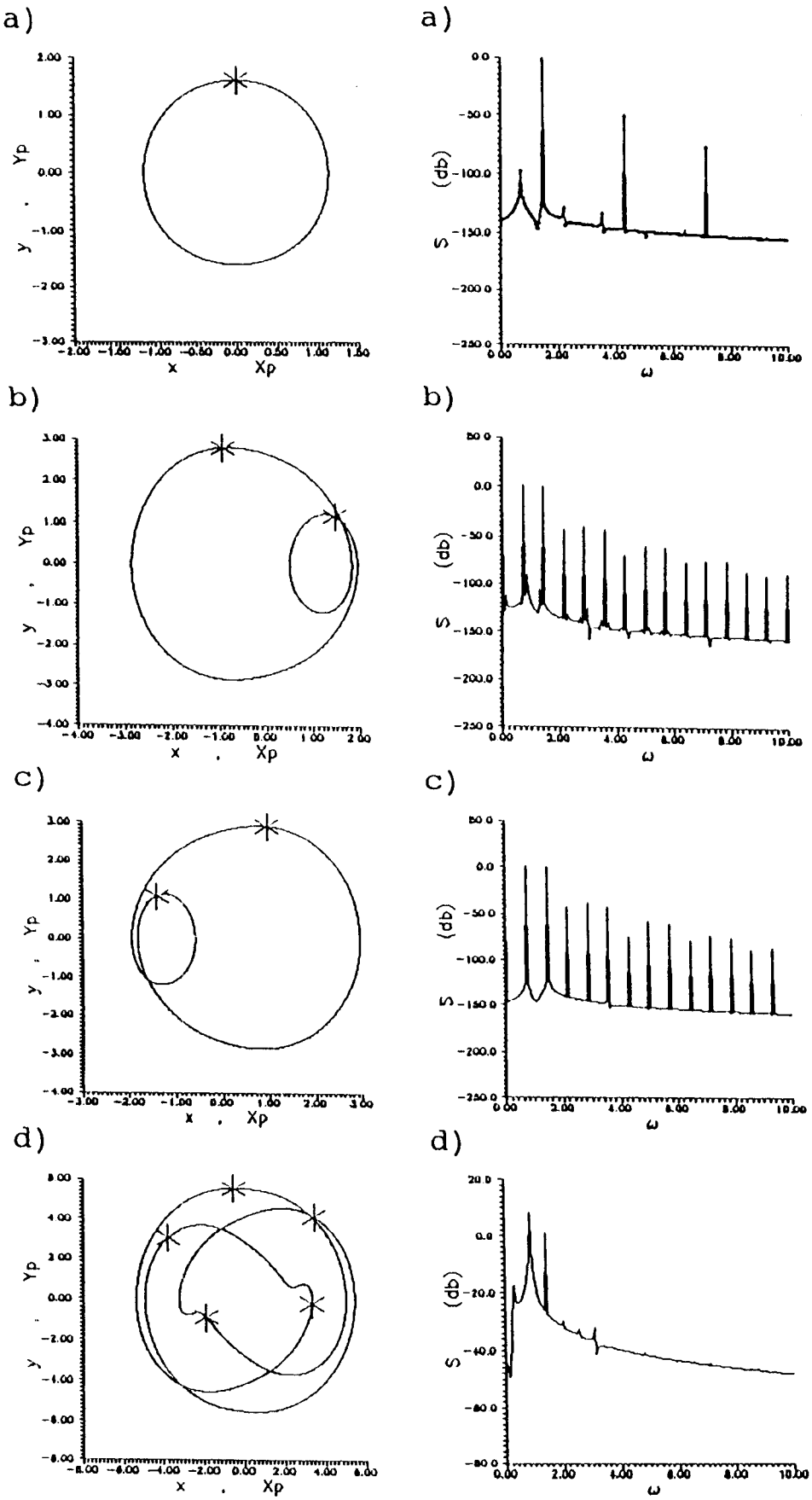


**Fig. 12.** Coexistence of multiple solutions (phase plane, power spectra) ($\alpha = 1$, $\beta = 0$, $\delta = 0{\cdot}01$, $f_0 = 0$, $f_1 = 2$, $\omega = 1{\cdot}43$) Initial conditions $[x(0), y(0)]$: (a) $T[0,0]$, (b) $2T[-1,0]$, (c) $2T[1,1]$, (d) $5T[-3,1]$.

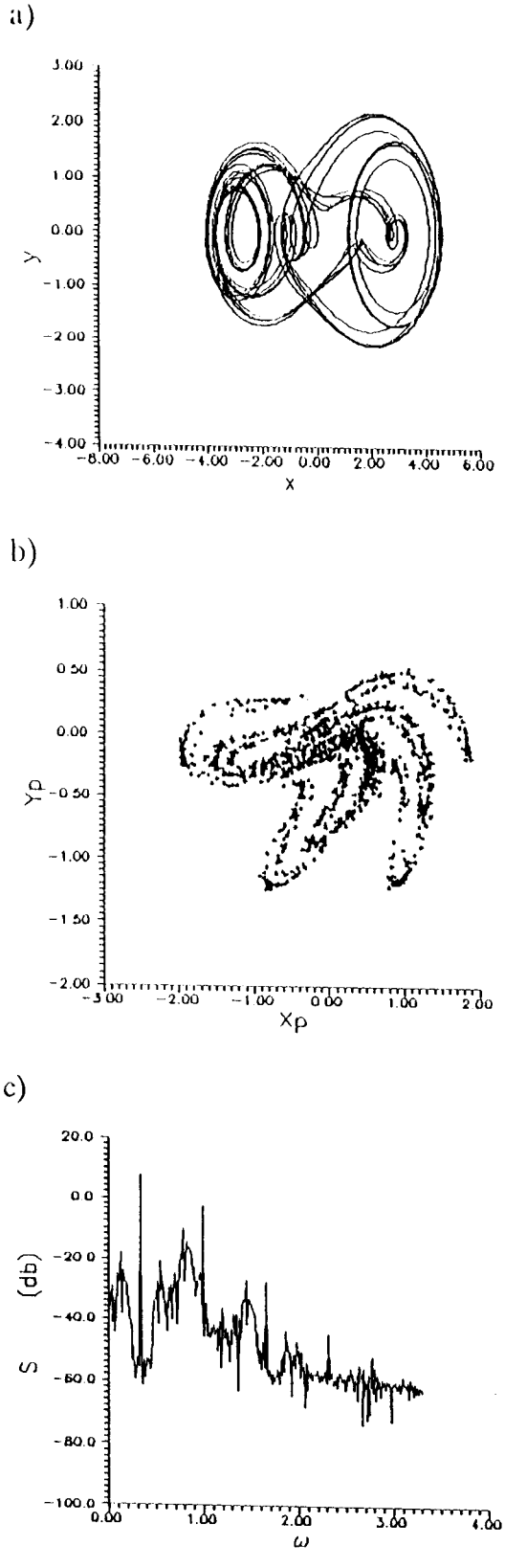


**Fig. 13.** Chaotic attractor via period doubling: (a) phase plane, (b) Poincaré Map, (c) power spectra ($\alpha = 1$, $\beta = 0$, $\delta = 0{\cdot}01$, $f_0 = 0, f_1 = 2$, $\omega = 0{\cdot}335$).

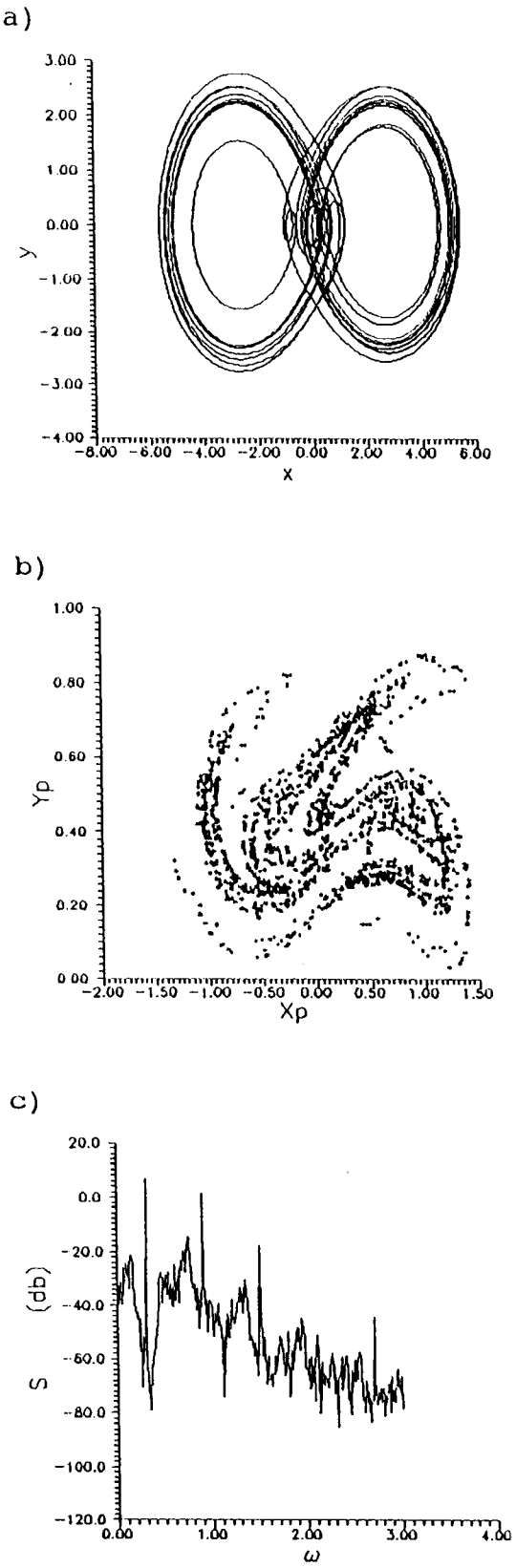


**Fig. 14.** Chaotic attractor via an explosion: (a) phase plane, (b) Poincaré Map, (c) power spectra ($\alpha = 1$, $\beta = 0$, $\delta = 0{\cdot}01$, $f_0 = 0, f_1 = 2$, $\omega = 0{\cdot}33$).

small amplitude waves combined with a steady current and a possible quasi-static representation of other nonsteady phenomena, induces 1/2 subharmonic response which can bifurcate and become chaotic. Wave excitation alone does not induce period doubling in the subharmonic region but creates a symmetry loss in the superharmonic region associated with the appearance of even resonances. This local bifurcation can lead to period doubling via an even ultra-subharmonic. Both secondary phenomena exibit large amplitude response coexisting with harmonic response.

The chaotic attractor found in the system excited by waves and current occurs for lower values of excitation amplitude than those of the system excited by waves alone. Consequently, the existence of even a weak current could generate a chaotic response of a vessel in a multi-point mooring configuration in a moderate sea state. This result is consistent with numerical evidence of period doubling in mooring systems and identifies the coupling of bias and periodic excitation as the generating mechanism of instability and sensitivity to initial conditions.

The semi-analytical method described in this study is found to be efficient for searching various types of complex nonlinear responses including coexisting multiple periodic solutions, and chaotic attractors corresponding to period doubling and explosions. Hence the method may supplant or significantly reduce the efforts of a numerical search in parameter space otherwise needed to complete the analysis of the strongly nonlinear ocean system considered.

## ACKNOWLEDGEMENTS

The authors gratefully acknowledge the financial support from the United States Office of Naval Research (Grant No. N00014-88-K-0729). The reviewers comments are also greatly appreciated.

## REFERENCES

1. Thompson, J.M.T., Complex dynamics of compliant offshore structures. *Phil. Trans. R. Soc. Lond., A.*, **387** (1983) 407–27.
2. Thompson, J.M.T., Bokaian, A. R. & Ghaffari, R., Subharmonic and chaotic motions of compliant offshore structures and articulated mooring towers. *J. Energy Resources Tech.*, **106** (1984) 191–8.
3. Papoulias, F.A. & Bernitsas, M.M., Autonomous oscillations, bifurcations and chaotic response of moored vessels. *J. Ship Res.*, **32** (1988) 220–8.
4. Bishop, S.R. & Virgin, L.N., The onset of chaotic motions of a moored semi-submersible. *J. Offshore Mech. Arctic Eng.*, **110** (1988) 205–9.
5. Sharma, S.D., Jiang, T. & Schellin, T.E., Dynamic instability and chaotic motions of a single-point moored taker. In *Proc. 17th ONR Symposium on Naval Hydrodynamics*, The Hague, National Academic Press, Washington D.C., 1988, pp. 543–63.
6. Virgin, L.N. & Bishop, S.R., Complex dynamics and chaotic responses in the time domain simulations of a floating structure. *Ocean Eng.*, **15** (1988) 71–90.
7. Gottlieb, O. & Yim, S.C.S., The onset of chaos in a multi-point mooring system. In *Proc. 1st European Offshore Mech. Symp.*, Vol. 1. Int. Soc. Offshore and Polar Enging (ISOPE), 1990, pp. 6–12.
8. Bernitsas, M.M. & Chung, J.S., Nonlinear stability and simulation of two-line ship towing and mooring. *App. Ocean Res.*, **11** (1990) 153–66.
9. Choi, H.S. & Lou, J.Y.K., Nonlinear behavior of an articulated loading platform. *App. Ocean Res.*, **13** (1991) 63–74.
10. Jiang, T., Investigation of nonlinear ship dynamics involving instability and chaos in examples from offshore technology. Institut fur Schiffbau, Universitat Hamburg, Report No. 512, 1991 (in German).
11. Ueda, Y., Steady motions exhibited by Duffing's equation: a picturebook of regular and chaotic motions. In *New Approaches to Nonlinear Problems in Dynamics*, ed. P. Holmes. Society of Industrial & Applied Mathematics (SIAM), 1980, pp. 311–22.
12. Ueda, Y., Explosion of strange attractors exibited by Duffing's equation. In *Nonlinear Dynamics*, ed. R.H.G. Helleman. 1980, pp. 422–34.
13. Parlitz, U. & Lauterborn, W., Superstructure in the bifurcation set of the Duffing equation. *Phys. Lett.*, **107A** (1985) 351–5.
14. Nayfeh, A.H. & Mook, D.T., *Nonlinear Oscillations*. Wiley, New York, 1979.
15. Guckenheimer, J. & Holmes, P., *Nonlinear Oscillations, Dynamical Systems and Bifurcation of Vector Fields*. Springer-Verlag, New York, 1986.
16. Burton, T.D. & Rahman, Z., On the multi-scale analysis of strongly nonlinear forced oscillators. *Int. J. Nonlinear Mech.*, **21** (1986) 135–46.
17. Szemplinska-Stupnicka, W., Secondary resonances and approximate models of routes to chaotic motions in nonlinear oscillators. *J. Sound Vib.*, **113** (1987) 155–72.
18. Rahman, Z. & Burton, T.D., Large amplitude primary and superharmonic resonances in the Duffing oscillators. *Int. J. Nonlinear Mech.*, **110** (1986) 363–80.
19. Szemplinska-Stupnicka, W. & Bajkowski, J., The 1/2 subharmonic resonance and its transition to chaotic motion in a nonlinear oscillator. *Int. J. Nonlinear Mech.*, **21** (1986) 401–19.
20. Hayashi, C., *Nonlinear Oscillations in Physical Systems*. McGraw-Hill, New York, 1964.
21. Szemplinska-Stupnicka, W., Bifurcations of harmonic solution leading to chaotic motions in the softening type Duffing's oscillator. *Int. J. Nonlinear Mech.*, **23** (1988) 257–77.
22. Nayfeh, A.H. & Sanchez, N.E., Bifurcations in a forced softening Duffing oscillator, *Int. J. Nonlinear Mech.*, **24** (1989) 483–97.
23. Skop, R.A., Mooring systems: a state of the art review. *J. Offshore Mech. Arctic Eng.*, **110** (1988) 365–72.
24. Leonard, J.W., *Tension Structures*. McGraw-Hill, New York, 1988.
25. Sarpkaya, T. & Isaacson, M.M., *Mechanics of Wave Forces on Offshore Structures*. Van Nostrand Reinhold, New York, 1981.
26. Newman, J.N., *Marine Hydrodynamics*. MIT Press, Cambridge, MA, 1977.
27. Patel, M.H., *Dynamics of Offshore Structures*. Butterworths, London, 1989.

28. Jiang, T., Schellin, T.E. & Sharma, S.D., Maneuvering simulation of a tanker moored in a steady current including hydrodynamic memory effects and stability analysis. RINA *Proc. Int. Conf. on Ship Manoeuvrability*, (1987) **1**, paper 25, 1–12.
29. Bernitsas, M.M. & Papoulias, F.A., Stability of single point mooring systems. *App. Ocean Res.*, **8** (1986) 49–58.
30. Papoulias, F.A. & Bernitsas, M.M., Stability of motions of moored ocean vehicles. *Dynamics and Stability of Systems*, **4** (1986) 323–41.
31. Jiang, T. & Schellin, T.E., Motion prediction of single-point moored tanker subjected to current, wind and waves. *J. Offshore Mech. Arctic Eng.*, **112** (1990) 83–90.
32. McKenna, H.A. & Wong, R.K., Synthetic fiber rope, properties and calculations relating to mooring systems. In *Deepwater Mooring and Drilling*, ASME, New York, **7**, 1979.
33. Papoulias, F.A., Dynamic analysis of mooring systems, PhD Dissertation, The University of Michigan, 1987.
34. de Kat, J.O. & Wichers, E.W., Behavior of a moored ship in unsteady current, wind and waves. *Mar. Tech.*, **28** (1991) 251–64.
35. Fujino, M. & Sagara, N., An analysis of dynamic behavior of an articulated column in waves — effects of nonlinear hydrodynamic drag force on the occurrence of subharmonic oscillation. *J. Japan Society of Naval Architects*, **167** (1990) 103–12 (in Japanese).
36. Wichers, J.E.W., A Simulation Model for a Single Point Moored Tanker, MARIN (Pub. no. 797), Maritime Research Inst, Netherlands, Wageningen, The Netherlands, 1988.
37. Schellin, T.E., Jiang, T. & Sharma, S.D., Motion simulation and dynamic stability of an ancored tanker subject to current, wind and waves. *J. Ship Tech. Res.*, **37** (2)(1990) 64–84.
38. Nayfeh, A.H. & Khdeir, A.A., Nonlinear rolling of ships in regular beam seas. *Int. Shipbldg Prog.*, **33** (1986) 40–9.
39. Nayfeh, A.H. & Khdeir, A.A., Nonlinear rolling of biased ships in regular beam waves. *Int. Shipbldg Prog.*, **33** (1986) 84–93.
40. Witz, J.A., Ablett, C.B. & Harrison, J.H., Roll response of semi-submersibles with nonlinear restoring moment characteristics. *App. Ocean Res.*, **11** (1989) 153–66.
41. Falzarano, J.M. & Troesch, A.W., Application of modern geometric methods for dynamical systems to the problem of vessel capsizing with water on deck. In *Proc. 4 Int. Conf. Stability of Ships and Ocean Vehicles*, Naples, Italy, 1990.
42. Falzarano, J.M., Predicting complicated dynamics leading to vessel capsizing. PhD Dissertation, The University of Michigan, 1990.
43. Pauling, J.R., An equivalent linear representation of the forces exerted on the OTEC cold water pipe by combined effects of waves and current. Ocean Engineering for OTEC, Proceedings of a Special Conference: 1980 Energy Sources Technology Conference. ed. O.M. Griffith, ASME, New York. 21–28, 1980.
44. Hagedorn, P., *Nonlinear Oscillations*. Oxford University Press, Oxford, 1978.
45. Holmes, P., A nonlinear oscilator with a strange attractor. *Philos. Trans. R. Soc.*, **A292** (1979) 419–48.
46. Thompson, J.M.T. & Stewart, H.B., *Nonlinear Dynamics and Chaos*. Wiley, Chichester, 1986.
47. Ioos, G. & Joseph, D.D., *Elementary Stability and Bifurcation Theory*. Springer-Verlag, New York, 1981.
48. Feigenbaum, M.J., Universal behavior in nonlinear systems. *Los Alamos Sci.*, **1** (1980) 4–27.
49. Grebogi, C., Ott, E. & York, J.A., Crises, sudden changes in chaotic attractors and transient chaos. *Physica D*, **7** (1983) 181–200.

## APPENDIX

$$G_i(A_k, \Phi) = 0$$

### Wave and current excitation: unsymmetric solution

$$(i,k) = (3,1) \Rightarrow x_0(t) = A_0 + A_1 \cos(\omega t + \Phi)$$

$$R_2[R_1 S_0 S_1 + 2R_0(1 + S_0^2 + \tfrac{1}{4}S_1^2)] = 0 \tag{A1}$$

$$R_0 R_1 (1 + S_0^2 + \tfrac{3}{4}S_1^2) + [R_0^2 + \tfrac{1}{4}(3R_1^2 + R_2^2) - \alpha^2] S_0 S_1 = 0 \tag{A2}$$

$$2R_0 R_1 S_0 S_1 + (R_0^2 - \alpha^2)(1 + S_0^2 + \tfrac{1}{2}S_1^2) + \alpha^2 \tfrac{1}{2}(R_1^2 - R_2^2)(1 + S_0^2) + \tfrac{1}{8}(3R_1^2 + R_2^2)S_1^2 = 0 \tag{A3}$$

where

$$R_0 = \omega_0^2[A_0 + \beta \operatorname{sgn}(x_0)] - f_0$$
$$R_1 = (\omega_0^2 - \omega^2)A_1 - f_1 \sin \Phi$$
$$R_2 = -\delta\omega A_1 + f_1 \cos \Phi$$
$$S_0 = A_0 + \beta \operatorname{sgn}(x_0)$$
$$S_1 = A_1$$

and

$$\omega_0^2 = \frac{\alpha}{\sqrt{1 + \beta^2}}$$

### Wave excitation: symmetric solution

$$(i,k) = (2,1) \Rightarrow x_0(t) = A_1 \cos(\omega t + \Phi)$$

$$[(\tfrac{3}{2}\omega_0^2 - \omega^2)A_1^2 - f_1 A_1 \sin \Phi + 2\omega_0^2(1 + \beta^2)](f_1 \cos \Phi - \delta\omega A_1) = 0 \tag{A4}$$

$$A_1\{\tfrac{3}{4}[(\omega_0^2 - \omega^2)A_1 - f_1 \sin \Phi]^2 + \tfrac{1}{4}(f_1 \cos \Phi - \delta\omega A_1)^2 + \omega_0^4\beta^2 - \alpha^2\} + \omega_0^2[(\omega_0^2 - \omega^2)A_1 - f_1 \sin \Phi](1 + \beta^2 + \tfrac{3}{4}A^2) = 0 \tag{A5}$$